Scientific paper

Encapsulation of Dirhenium(III) Carboxylates into Zirconium Phosphate

Anastasiia Slipkan,[1,2] Nataliia Shtemenko,[1,2] Dina Kytova[1,2] and Alexander Shtemenko*[,1]

[1] *Ukrainian State University of Chemical Technology, Gagarin Ave. 8, Dnipro, Ukraine, 49005*

[2] *Dnipro University of Technology, Dmytro Yavornytskiy Ave. 19, Dnipro, Ukraine,49005*

** Corresponding author: E-mail: shtemenko@ukr.net*
Tel.+380 (97) 392 91 52

Received: 08-27-2019

Abstract

Present work reports the synthesis of zirconium phosphate nanoparticles containing dirhenium(III) substance bis-dimethylsulfoxide-cis-tetrachlorodi-μ-pivalatodirhenium(III) with formula *cis*-$Re_2(C(CH_3)_3COO)_2Cl_4 \cdot 2DMSO$ (**I**) and θ-zirconium phosphate with formula θ-$Zr(HPO_4)_2 \cdot 6H_2O$ (ZrP). The intercalation process was monitored by EAS. Due to the spectral characteristics of the quadruple bond the conclusion was made that the obtained intercalated compounds had *cis*-configuration of ligands around cluster dirhenium fragment. The proposed mechanism of intercalation includes the substitution of the axial ligands of **I** by phosphate groups of ZrP first on the surface of ZrP, than in the inner layers. Two received products of the intercalation were characterized by SEM, XRPD, FT-IR, TGA analysis witnessing about successful intercalation process. The formation of new phases with interlayer distances of 10.53–16.6 Å was found, the average size of obtained platelets was 100–200 nm.

Keywords: Dirhenium(III) carboxylates, zirconium phosphate, nanoparticles, intercalation.

1. Introduction

Layered Zr(IV) phosphates ZrP with α, β, γ and θ-structures, α-$Zr(HPO_4)_2 \cdot H_2O$, β-$Zr(HPO_4)_2 \cdot 2H_2O$, θ-$Zr(HPO_4)_2 \cdot 6H_2O$ and γ-$ZrPO_4 \cdot H_2PO_4 \cdot 2H_2O$ are well known as convenient, long storing and non-toxic preparations, that due to labile protons of POH groups can be used for many chemical processes. [1,2,3] ZrP is one of the most studied inorganic cation exchange material with high thermal stability, solid-state ion conductivity, resistance to ionizing radiation and is known as a host capable to incorporate different types of guest molecules.[4]

Crystal structure of ZrP presents a lattice with Zr^{4+} ions bonding to oxygen atoms from three different phosphate groups producing covalently connected three-dimensional cross-linked planes. The fourth oxygen atom of the tetrahedral phosphate group is protonated and points towards the interlayer space. Water molecules in the interlayer space form hydrogen bonds with hydroxyl groups and are perpendicular to the layer. θ-ZrP is a hydrated phase of α-ZrP and has a similar structure to the α-ZrP with five additional water molecules in the interlaminar space, thus the distance between the layers increases up to 10.3 Å (Fig. 1A). (Fig. 1A)

Upon dehydration, θ-ZrP is converted to α-ZrP (the distance between the layers is 7.6 Å) without the formation of any other intermediate phase.[5] The efficiency of intercalation to all types of ZrP depends on the distance between the layers and the size of intercalated molecules.[6] Cations (less than 2.63 Å) or small molecules can be intercalated within the layers of α-ZrP. However, the intercalation of large cations here was very low. Due to the larger interlaminar space θ-ZrP can include large molecules and cations, such as insulin and others[6,7]. That is why among the described modification of ZrP we chose θ-ZrP for our study. It was shown that differences in properties (solubility, charge, polarity) substances such as doxorubicin, insulin, amino acids and various organometallic complexes could be intercalated into ZrP layers.[5,6,8–13]

Dirhenium(III) carboxylates with the unique quadruple bond were described as anticancer, anti-anemic, nephro- and hepato-protecting substances, possessing mighty antioxidant properties due to δ-bond unsaturation.[14–17] Being nontoxic, these compounds present a perspective platform

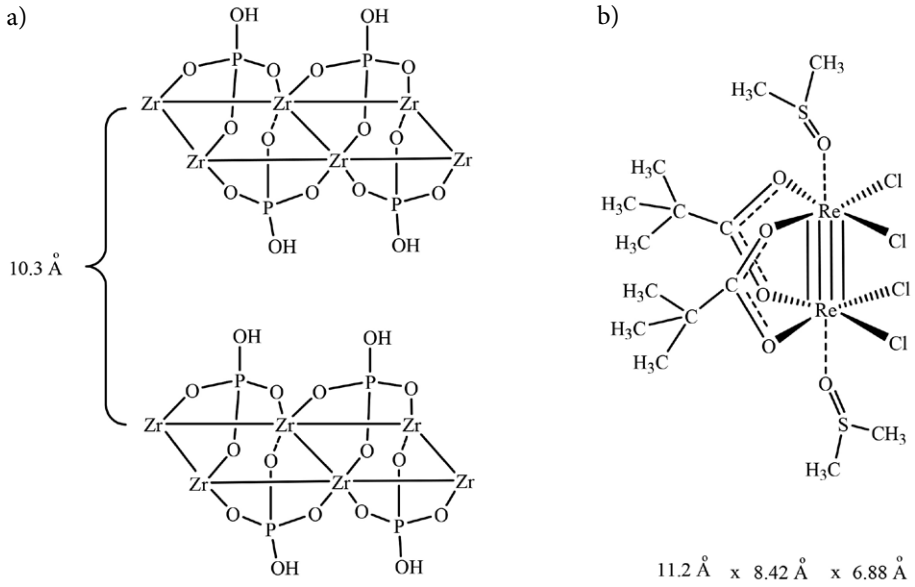

Fig. 1 Structure of $Zr(HPO_4)_2 \cdot 6H_2O$ (θ-ZrP) (a) and *cis*-$Re_2(C(CH_3)_3COO)_2Cl_4 \cdot 2DMSO$ (**I**) (b) with linear dimensions.

for the creation of a new class of Re-containing medicines. Bis-dimethylsulfoxide-cis-tetrachlorodi-μ-pivalatodirhenium(III) of common formula *cis*-$Re_2(C(CH_3)_3COO)_2Cl_4 \cdot 2DMSO$ (**I**) and structure shown on the Fig.1B was studied in the model of tumor-growth and showed essential antioxidant and anticancer activities as a component of the antitumor rhenium-platinum antitumor system.[18,19] Among them the substances with superoxide dismutase activity and abilities to interact with proteins were found. The valuable biological properties of these compounds were better realized in the forms of liposomes, than in water solutions,[20,21] that occurred due to lipid layer protection of dirhenium substances from hydrolysis and also by existing of the equilibrium inside the liposome, that enhanced chemical potential of the preparations. Thus, the approach to create nanocarriers for delivery of the quadruple-bonded complexes is very promising.

The ZrP nanoplatelets may be prepared by methods of intercalation or exfoliation [22]. The last method had some disadvantages, for example, the necessity of the preintercalator, which may be toxic. That's why we consider it reasonable to use the intercalation procedure.

Thus, taking into account all the above, the aim of the present work was to investigate the process of intercalation of *cis*-$Re_2(C(CH_3)_3COO)_2Cl_4 \cdot 2DMSO$ (**I**) into θ-ZrP and to obtain **I**/ZrP nanoplatelets by intercalation method.

2. Experimental Section

2. 1. Materials and Methods

All used chemicals were of analytical grade purity. θ-ZrP was obtained according to [5] with some modifications (see below). *cis*-$Re_2(C(CH_3)_3COO)_2Cl_4 \cdot 2DMSO$ (**I**) was obtained according to.[16]

2. 2. Synthetic Methods

Synthesis of θ-ZrP: 200 ml of 0.05 M water solution of $ZrOCl_2 \cdot 8H_2O$ was added to preheated up to 94 °C 200 ml of 6 M H_3PO_4 in a 500 ml round bottom flask. The resulting solution was constantly stirred at 94°C for 48 h. The product was a crystalline precipitate centrifuged and washed several times with water.

*Synthesis of **I**/θ-ZrP composites*. The process of intercalation of **I** in θ-ZrP was conducted in isopropyl alcohol (IPA), not in the water, to avoid possible hydrolytic processes of dirhenium(III) complexes. First, the suspension of **I** and θ-ZrP in IPA in the molar ratios of **I** and θ-ZrP 1:5 and 1:30 was prepared: the required amount of θ-ZrP was suspended in $5.0 \cdot 10^{-3}$ M solution of **I.** The molar ratios of **I**/θ-ZrP 1:5 and 1:30 were taken according to the similar investigations of the intercalation process between θ-ZrP and platinides.[23] Then the suspension was stirred vigorously at 60 °C for 5 days. The intercalation process was controlled by each day measurements of pH and UV-Vis absorption spectra (EAS) of the supernatant of a centrifuged aliquot. Constant pH and UV-Vis absorbance indicated the end of the intercalation process. The reaction mixture was cooled, centrifuged (micro-centrifuge type 320; Mechanika Precyzyjna, Poland) at 14000xg, filtered, washed three times with IPA, dried and weighted. As a result of the intercalation, the mass of the I/θ-ZrP of 1:5 and 1:30 molar ratio increased on 0.57 g (26% of the substance was intercalated) and 1.45 g (66% of the substance was intercalated) correspondingly.

2. 3. Measurements

pH was controlled by pH-meter-millivoltmeter pH-150 MA. UV-vis absorption spectra were measured

in IPA using spectrophotometer "Specord M-40" (Germany).

Calculations of three-dimension structures and linear dimensions were made with the help of the Mercury (Mercury for Windows, version 3.6 using the crystal structure of **I** [16]) program for crystal structure visualization, exploration and analysis.

Scanning electron micrographs (SEM) of the samples were performed using a Tescan Mira 3 LMU scanning electron microscope at an acceleration voltage of 30 kV. Samples were prepared using Digiprep 251 and MicraCut 151 (Metkon). The speed of rotation of the disk – 50–600 rpm, the speed of rotation of the samples 50–150 rpm.

Zeta potentials of ZrP nanoplatelets were determined using Zeta Sizer Nano S (Malvern, UK) at 25 °C at pH 7.4.

X-ray diffraction (XRPD) measurements were performed from 5 to 60 °C using X-ray diffractometer PANalytical X'Pert High Score with a copper anode source ($K_{\alpha 1}$, λ = 1.5406 Å).

IR spectra were recorded in the range of the 4000–400 cm^{-1} in dehydrated KBr tablets in infrared spectrophotometer FT-IR Spectrum BX, (Perkin Elmer).

Thermogravimetric analysis (TGA analysis) was conducted on the derivatograph Q-1500D Paulik-Paulik-Erday on the air in the interval 20–1000 °C with the speed 10 °C/min of temperature changing. α-Al_2O_3 served as an etalon. The error in determined temperature intervals was not more than 5%. After that, another modification of thermal destruction investigation, i.e. method of thermal exposures was used. The weighted sample of the substance was placed in the glass reactor for thermal exposures and was heated in an inert atmosphere under the temperatures of earlier determined temperatures of the weight losses during 4 h. After each exposure, the sample was weighed and the weight loss was determined.

The drug encapsulation efficiency (EE) of the composites was measured by spectrophotometric method according to[2] at different time intervals at 14900 cm^{-1} using Eq. (1):

$$EE(\%) = [(\text{Total } \mathbf{I} - \mathbf{I} \text{ in supernatant}) / \text{Total } \mathbf{I}] \times 100\% \quad (1)$$

3. Results and Discussion

3. 1. Spectral Investigation of Intercalation I with ZrP.

Spectral analysis was used by us to investigate interactions of different types of dirhenium cluster compounds with 1-palmitoyl-2-oleylphosphatidylcholin (POPC) preparation of liposomes,[20,24] proteins[25] and zirconium phosphate[26,27] due to ability of the quadruple bond to absorb in the visible area.

Different structural types of Re_2^{6+} derivatives had the characteristic absorption maxima in the visible area, the position of which were dependent from the quantity of hyperconjugated cycles around Re_2^{6+} center. The effect of hyperconjugation was realized due to the interaction of the delocalized π-bond of μ-carboxylic ligands group and the δ-component of the quadruple Re-Re bond. If dichlorotetra-μ-isobutiratodirhenium(III) $Re_2(i\text{-}PrCOO)_4Cl_2$ had

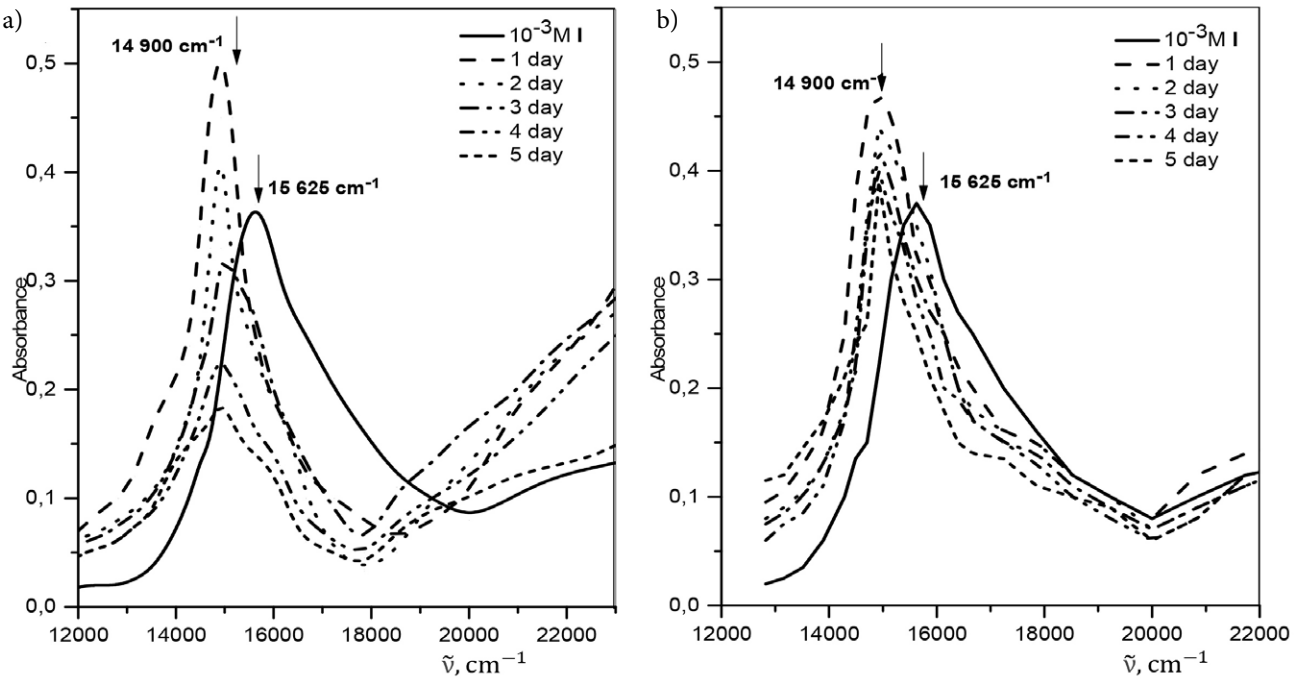

Fig. 2 EAS of the reaction mixture of **I** (10^{-3}M) and ZrP in IPA: a) at 1:30 ratio over time; b) at 1:5 ratio over time; control – IPA

maximum absorption in the area 20000 cm^{-1}, the bidentate coordinated tetra-μ-phosphates $[Re_2(HPO_4)_4(H_2O)_2]^{2-}$ and $[Re_2(HPO_4)_2(H_2PO_4)_2(H_2O)_2] \cdot 4H_2O$ had the δ→δ* absorption band at 15625 cm^{-1}. The replacement of carboxylic ligands on phosphate or chlorine groups would shift the absorption band δ→δ* to low energy region (bathochromic shift). So, the analogical spectral picture was expected to be seen in the present experiment.

Before starting the experiment, two important measurements were done: 1. The spectrum of ZrP in IPA was investigated, and no absorption in the area 12000–22000 cm^{-1} was detected; 2. The solution of **I** in IPA in concentration 10^{-3}M was heated at 60 °C during 5 days with spectral investigations and it was found that the intensity of the characteristic band of **I** (15625 cm^{-1}) was not changed. These measurements supported the idea, that any changes in the investigated area of the spectrum should be the reason of **I** and ZrP interactions.

On figure 2, EAS of the reaction mixtures of **I** with ZrP at 1:30 and 1:5 molar ratio over time are presented.

In both variants of the experiment, the sharp increase of intensity of the characteristic bond was noticed together with the shift from 15625 cm^{-1} to 14900 cm^{-1} that definitely indicated that there was an interaction of **I** with ZrP and formation of new complexes of **I** with phosphate groups from ZrP (**I**/ZrP) on the surface layers. Then the decrease of the intensity of the band 14900 cm^{-1} took place. To our mind, during the following process of intercalation, the concentration of **I** decreased due to penetration of **I** to interlayer space of ZrP. As more molecules of **I** penetrated to interlayer space and formed new complexes, as more the equilibrium **I** + ZrP ↔ **I**/ZrP was shifted to the side of the intercalation and formation of new complexes and accordingly we watched the decreasing of the characteristic band 14900 cm^{-1}.

Earlier it was shown by us, that dicarboxylates of dirhenium(III) reacted with POPC by substitution of axial chlorine groups on phosphate groups.[20,24] In our experiment we investigated the little bathochromic shift in the area of quadruple bond absorption that may propose the substitution of the carboxylic groups by phosphate from ZrP. But, it was proved, that dicarboxylates reacted with POPC by another type, i.e. by substitution of chlorine atoms on phosphate groups.[20,24]

The interaction of dicarboxylates with POPC was followed by a decrease of the bands 15400–15700 cm^{-1} and concomitant appearance of a new band at 12133 cm^{-1}, the intensity of which increased dramatically with time.[24] These two features are characteristics of a $Re_2(\delta) \rightarrow Re_2(\delta^*)$ electron transition for trans-dicarboxylates.[15] The process possibly involves the substitution of the chloride groups of dicarboxylates by POPC via oxygen atoms from the phosphate groups which initiates a cis-trans rearrangement of the bridging carboxylate ligand.

In our experiments, we did not detect the appearance of absorption in the area 12000 cm^{-1} that confirmed another mechanism of interaction without the formation of *trans*-product. Thus, the possible explanation of the spectral characteristic of the reaction mixture is the substitution of the DMSO in **I** by phosphate groups of ZrP without the formation of trans-derivatives and the only obtained product is the presented one on the Fig. 3 with remained *cis*-configuration.

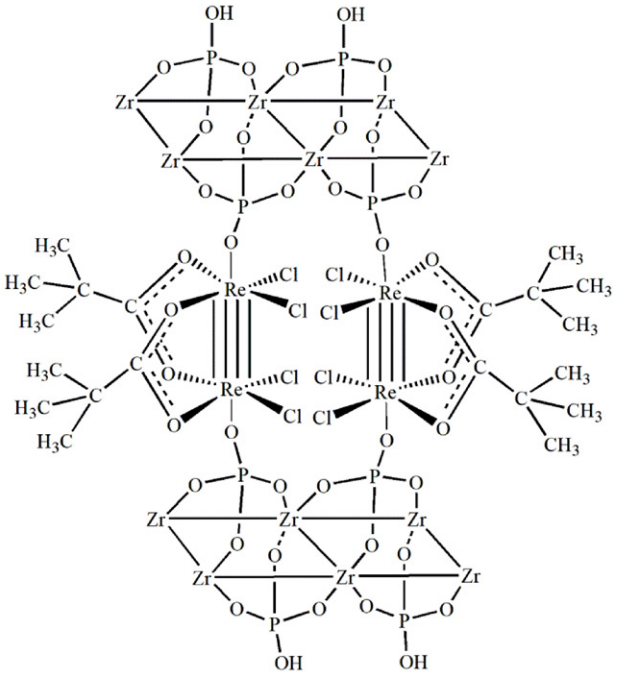

Fig. 3 The proposed formula of the product of the reaction between **I** and phosphate groups on the surface layers of ZrP

It is necessary to note, that the quadruple bond between two rhenium atoms has unique spectral properties: first to absorb in the visible area due to the δ→δ* transition of the spectrum, where no other organic molecules can absorb; second very important property of the band is the dependence of absorption from the number of organic ligands around cluster Re_2^{6+} fragment and their orientation. These two facts make it possible to demonstrate the mechanism of intercalation of the dirhenium(III) compound, which includes the modification of ZrP surface due to the coordination of its phosphate groups to the Re-Re core at first. Then the intercalation took place in ZrP inner layers. As to our knowledge, such mechanisms have not been shown yet for any intercalated substance.

3. 2. SEM

The SEM images of **I**/ZrP intercalation product 1:30 and 1:5 showed that hexagonal like shape of initial ZrP was stored (Fig. 4).

The average diameter of platelets is 104 nm for 1:30 adduct (Fig. 4A) and 120 nm for 1:5 adduct (Fig. 4B). The thickness for them is approximately 15.7 nm and 24.5 nm accordingly (Fig.4 C, D).

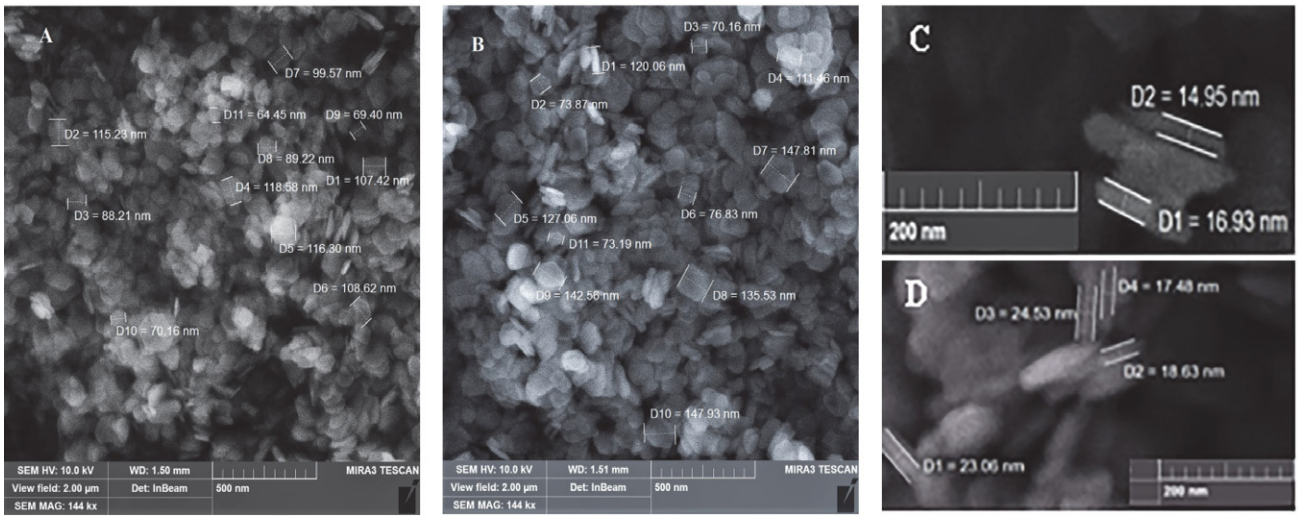

Fig. 4 The SEM images of the **I**/ZrP: A, C – 1:30, B,D – 1:5

Since the phosphate groups of ZrP are directed down and up relative to the plane, the rhenium(III) complex can coordinate on the surface of the nanoparticles as well. Such surface modification of ZrP with I was proved by EDX of intercalated material. Fig. 5 shows that the EDX spectrum for the I/ZrP intercalated product includes the characteristic peak indicating the presence of Re (8.1%) on the surface of the nanoparticles.

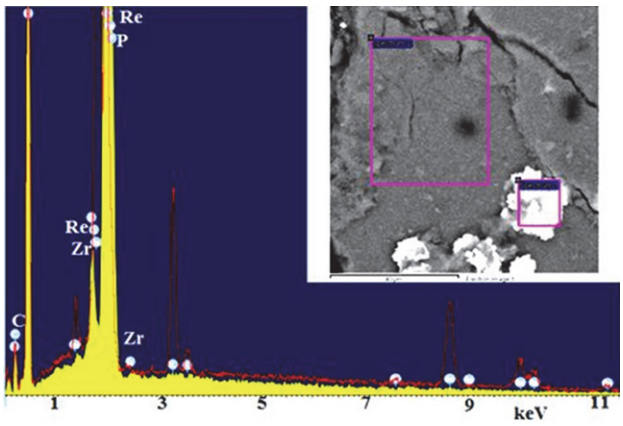

Fig. 5 EDX spectrum of I/ZrP 1:5

Zeta potential of both preparations **I**/ZrP is –37±2 mV showing that obtained nanoplatelets are stable in an aqueous medium.[12] The obtained nanoparticles have a platelet-like shape. Such shapes were shown to have some advances in comparison to spherical ones due to better adhesion, margination and binding properties. For example, the binding probability of nanorods was found to be three times higher than that of nanospheres with the same volume.[28] The obtained SEM data together with spectral investigations point that ZrP can be used as a matrix for cluster rhenium(III) with *cis*-configuration of carboxylate ligands.

3. 3. X-ray Powder Diffraction

The reaction of intercalation of **I** into interlayers is topotactic,[6] i.e. solid-phase reaction during which the packaging of atoms in the crystal of the reagent is practically the same, only distances between some atoms in several directions are changing. The diffraction peaks at the lowest 2θ angle correspond to the interlayer distance which depends on the intercalated substance.[29] The XRPD patterns of **I**/ZrP for molar ratios 1:30 and 1:5 show the appearance of new peaks (Fig. 6 B, C), indicating the formation of new phases.

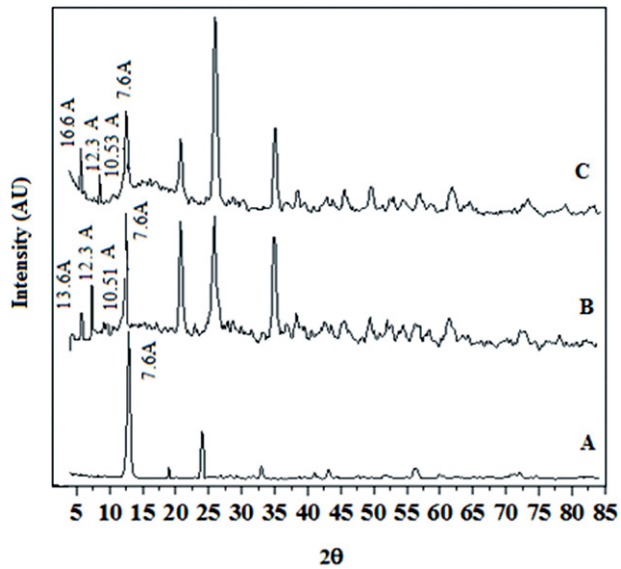

Fig. 6 X-ray diffraction α-ZrP (A), **I**/ZrP 1:30 (B) and **I**/ZrP = 1:5 (C)

In the absence of intercalated substances, the distance between layers of α-ZrP corresponds to 7.6 Å (Fig. 6A). The presence of this peak in the diffraction patterns of the intercalation products indicates that formed phases are

mixed. The intensity of this peak is lower in patterns B and C than in A, pointing to the reduction of this phase with increasing concentration of **I**.

Formations of new phases are followed with appearance of first-order diffraction peak 13.59 Å for **I**/ZrP 1:30 (Fig. 6B) and 16.6 Å for **I**/ZrP = 1:5 (Fig. 6C); besides, both composites show the second and the third peaks: 12.28 Å and 10.53 Å for **I**/ZrP 1:30 (Fig. 6B); 12.3 Å and 10.51 Å for **I**/ZrP = 1:5 (Fig. 6C).

Three-dimensional structure and lineal dimensions of **I** are presented on Fig. 7.

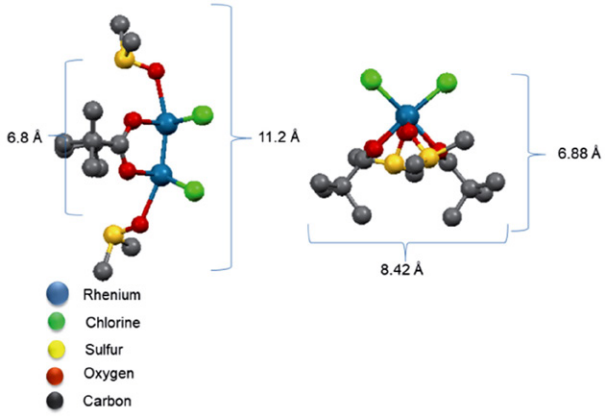

Fig. 7 Structure of **I** showing its dimensions as calculated by Mercury

If lineal dimensions for **I** molecule are known 11.2 x 8.42 x 6.88 Å3 and are presented on the Fig. 7, and interlayer distance in ZrP is also known to be 6.6 Å, this allows us to predict the interlayer distances in the newly formed phases and approximate coordination of the **I** molecules between ZrP layers. For instance, for **I**/ZrP 1:30 the shown interlayer distance 13.59 Å may correspond to disposition of **I** molecules parallel to ZrP layers (6.88 Å + 6.6 Å = 13.48 Å); accordingly the diffraction peak 16.6 Å may correspond to perpendicular disposition of **I** to ZrP layers (11.2 Å + 6.6 Å = 17.8 Å). A little decrease between calculated and real distances may be explained by compressing of ZrP layers and/or by hiding (interaction) of branched ligands of **I** into so-called "pockets" of ZrP.[6]

Thus, the analysis of XRPD patterns of newly synthesized **I**/ZrP products gives confirmation about the formation of new intercalated products and imagination about a possible disposition of **I** between layers of ZrP.

3. 4. FT-IR Data.

The obtained FT-IR data for **I**/ZrP 1:30 and 1:5 were identical, so we demonstrate data only for the first one in comparison with primary substances (Fig. 8).

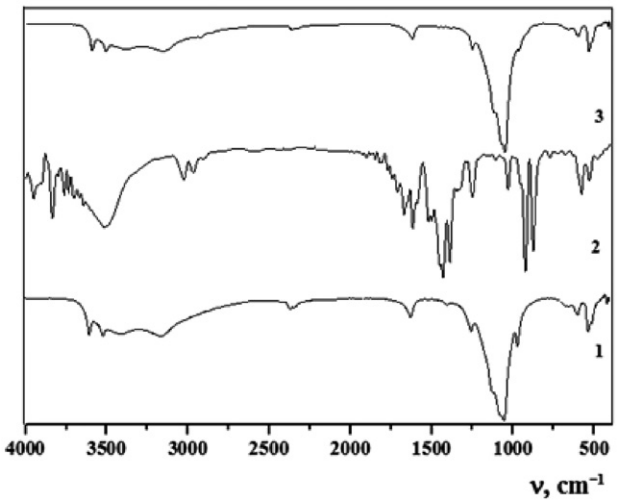

Fig. 8 FT-IR spectra of ZrP (1); **I** (2); **I**/ZrP 1:30 (3)

The data presented in the table and in the Fig.8 show the disappearance of the absorption bands in **I**/ZrP 1:30 characteristic for **I** structure, indicating that **I** is absent on the surface of the composite and support the earlier speculations about successful intercalation procedure. The only difference in spectra of initial ZrP and the complex **I**/ZrP is the absence of the band 1100–940 cm^{-1} in the last one referred to fluctuations of phosphate groups that may occur due to involvement of phosphate groups in the reaction.

3. 5. TGA Analysis.

Thermograms of both intercalation products show three weight losses (Fig.9).

First weight loss under 120°C corresponds to the loss of coordinated water in zirconium phosphate; the second

Table 1: Characteristic frequencies (cm^{-1}) and their correspondence in the FT-IR spectra of **I**, ZrP and **I**/ZrP 1:30

Substance	$\nu_s(CO)$	δ_{as}, ν_s $(C(CH_3)_3COO-)$	$\nu_s(H_2O)$, $\nu_s(OH-)$	ν_s *(DMSO)*	$\nu_s(P-O)$, $\nu_s(P-OH)$	$\nu_s(M-O)$
I	1420	2800 1470–1430	3500	1225–980	–	390–480
ZrP	–	–	1620 3500	– –	1200 1100–940	522
I/ZrP 1:30	–	–	1620 3500	–	1200	522

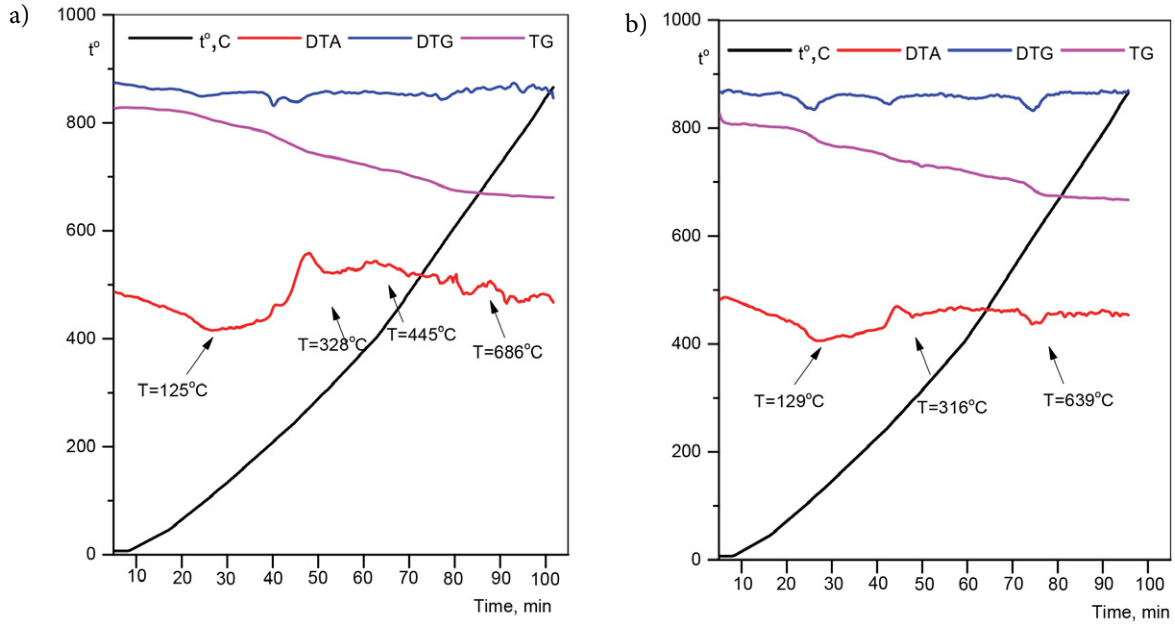

Fig. 9 Thermograms of **I**/ZrP: a) **I**/ZrP 1:5; b) **I**/ZrP 1:30.

under 250–350 °C – to the thermo destruction of **I** with the formation of the trans-isomer;[30] and the third – to condensation of phosphate groups and the formation of zirconium pyrophosphate. [31]

The weight losses in the first and second stages of thermograms for the **I**/ZrP 1:5 were: 9%; 13.2% (Fig. 9A) and for the **I**/ZrP 1:30 9%; 10% (Fig. 9B). Low levels of weight loss could be the result of quickly temperature increasing, so we decided to undertake another modification of thermal destruction investigation (see Materials and methods), i.e. method of thermal exposures. In this modification method following weight losses for the **I**/ZrP 1:5 were: 8.87% under 120 °C; 29.89% under 250–350 °C of heating and for **I**/ZrP 1:30 9.8% and 10.9% accordingly.

3. 6. Drug Loading Studies.

The time-depending drug encapsulation efficiency (EE) studies of **I**/ZrP 1:5 and **I**/ZrP 1:30 (Fig. 10) showed not so rapid uptake of **I** as it was found for example for curcumin (120 min).[2]

This may be explained by more necessary time for the reaction of substitution in comparison with time for the formation of hydrogen bonds between the hydroxyl groups of curcumin and negatively charged phosphate groups of ZrP. The maximum EE (66%) was reached only on the 5th day for **I**/ZrP 1:30 and 26% for **I**/ZrP 1:5.

Our further investigations are aimed at obtaining the mixed composites (for example **I** + cisplatin, or **I** + doxorubicin) and on studying their biological activities. This direction is very promising due to the following reasons: anticancer properties of solely introduced **I** and some alkyl carboxylates were not very essential, as it is known about introduction of other cytostatics; the group of Prof. A. Clearfield recently have shown good perspectives of ZrP composites as medicines[31,32] as in several biological models ZrP-composites were shown to be more active than free substances.

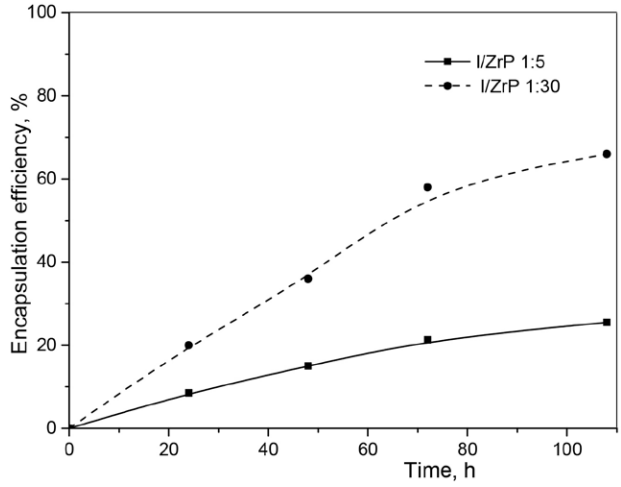

Fig. 10 Time-dependent **I** encapsulation efficiency of ZrP nanoplatelets

4. Conclusions

The method of intercalation of **I**, the representative of cis-carboxylate of dirhenium(III) compounds, into θ-ZrP was elaborated. The possible mechanism of intercalation is the substitution of the axial ligands by the layers phosphate groups to the cluster center Re_2^{6+} producing new phases with interlayer distances of 10.53–16.6 Å and the average size of platelets 100–200 nm. Two received

products of the intercalation process were characterized by appropriate methods. The existence of the quadruple bond in the structure of **I** made it possible to demonstrate the mechanism of intercalation of the dirhenium(III) compound. The obtained result is the starting point for the synthesis of mixed ZrP nanocarriers on the base of quadruple-bonding compounds with promising biological properties.

Acknowledgments

We are grateful to the Ministry of Education and Science of Ukraine (Grants 0107U000528 and 0111U000111) the studies were supported by.

5. References

1. W. J. Roth, B. Gil, W. Makowski, B. Marszaleka and P. Eliasova, *Chem. Soc. Rev.* **2016**, *45*, 3400–3438. **DOI:**10.1039/C5CS00508F
2. H. Kalita, B. N. Prashanth Kumar, S. Konar, S. Tantubay, M. Kr. Mahto and M. Mandal, *Mater. Sci. Eng: C.* **2016,** *60,* 84–91**.** **DOI:**10.1016/j.msec.2015.11.010
3. J. Gonzalez-Villegas, Y. Kan, V. I. Bakhmutov, A. Garcia-Vargas, M. Martinez, A. Clearfield and J. L. Colon, *Inorg. Chim. Acta*. **2017**, *468*, 270–279. **DOI:**10.1016/j.ica.2017.05.057
4. A. Diaz, V. Saxena, J. Gonzalez, A. David, B. Casanas, C. Carpenter, J. D. Batteas, J. L. Colon, A. Clearfield and M. D. Hussain, *Chem. Commun*. **2012**, *48*, 1754–1756. **DOI:**10.1039/c2cc16218k
5. A. A. Marti and J. L. Colon, *Inorg. Chem*. **2003**, *42***,** 2830–2832. **DOI:**10.1021/ic025548g
6. A. Diaz, A. David, R. Perez, M. L. Gonzalez, A. Baez, S. E. Wark, P. Zhang, A. Clearfield and J. L. Colon, *Biomacromolecules*. **2010**, *11***,** 2465–2470. **DOI:**10.1021/bm100659p
7. A. A. Marti, N. Rivera, K. Soto, L. Maldonado and J. L. Colon, *Dalton Trans.* **2007**, *17*, 1713–1718. **DOI:**10.1039/B618802H
8. A. Clearfield, R. H. Blessingt and J. A. Stynes, *J. Inorg, nucl. Chem*. **1968**, *30*, 2249–2258. **DOI:**10.1016/0022-1902(68)80224-6
9. U. Costantino, *J. Chem. Soc., Dalton Trans.* **1979**, *2*, 402–405. **DOI:**10.1039/dt9790000402
10. R. Backov, D. J. Jones and J. Roziere, *Chem. Commun*. **1996**, *1*, 599–600. **DOI:**10.1039/CC9960000599
11. F. Carn, A. Derre, W. Neri, O. Babot, H. Deleuze and R. Backov, *New J. Chem.* **2005**, *29*, 1346–1350. **DOI:**10.1039/b507960h
12. V. Saxena, A. Diaz, A. Clearfield and J. D. Batteas, M. D. Hussain, *Nanoscale*. **2013**, *5*, 2328–2336. **DOI:**10.1039/c3nr34242e
13. S. Shakshooki, B. E. Ali, S. El-Rais and M. El-Rais, *Am. J. Chem*. **2014**, *4*, 22–28.
14. N. Shtemenko, A. Shtemenko *Ukr. Biochem. J.*. **2017**, *89*, 5–26. **DOI:**10.15407/ubj89.02.005
15. N. Shtemenko, K. Domasevich, E. Zabitskaya and A. Golichenko, *J. Chem. Soc., Dalton Trans.* **2009**, *26*, 5132–5136. **DOI:**10.1039/b821041a
16. N. I. Shtemenko, H. T. Chifotides, K. V. Domasevich, A. A. Golichenko, S. A. Babiy, Z. Li, K. V. Paramonova, A. V. Shtemenko and K. R. Dunbar, *J. Inorg. Biochem.* **2013**, *129*, 127–134. **DOI:**10.1016/j.jinorgbio.2013.09.001
17. A. A. Golichenko, K. V. Domasevitch, D. E. Kytova and A. V. Shtemenko, *Acta Cryst.* **2015**, *71*, 45–47. **DOI:**10.1107/S2056989014026620
18. I. V. Leus, I. A. Klenina, K. A. Zablocka, A. A. Golichenko, A. V. Shtemenko and N. I. Shtemenko, *Biopolymers and Cell.* **2011**, *27*, 465–471. **DOI:**10.7124/bc.000119
19. K. L. Shamelashvili, N. I. Shtemenko, I. V. Leus, S. O. Babiy and O. V. Shtemenko, *Ukr. Biochem. J*. **2016**, *88*, 29–39. **DOI:**10.15407/ubj88.04.029
20. N. Shtemenko, O. Berzenina, D. Yegorova and A. Shtemenko, *Chem. Biodivers*. **2008**, *5*, 1660–1667. **DOI:**10.1002/cbdv.200890153
21. Y. Zhu, T. Shimizu, T. Kitajima, K. Morisato, N. Moitra, N. Brun, T. Kiyomura, K. Kanamori, K. Takeda, H. Kurata, M. Tafu and K. Nakanishi, *New J. Chem.* **2015**, *39*, 2444–2450. **DOI:**10.1039/C4NJ01749H
22. F. Xia, H. Yong, X. Han and D. Sun, *Nanoscale Res. Lett.* **2016**, 11, 1–7. **DOI:**10.1186/s11671-016-1559-6
23. E. J. Rivera, C. Figueroa, J. L. Colon, L. Grove and W. B. Connick, *Inorg.Chem.*, **2007**, *46*, 8569–8576. **DOI:**10.1021/ic7006183
24. Z. Li, N. I. Shtemenko, D. Y. Yegorova, S. O. Babiy, A. J. Brown, T. Yang, A. V. Shtemenko and K. R. Dunbar *J Liposome Res*. **2015**, *25*, 78–87. **DOI:**10.3109/08982104.2014.954127
25. I. V. Leus, I. O. Klenina, K. A. Zablotska, O. A. Golichenko, O. V. Shtemenko, N. I. Shtemenko *Biopolymers and Cell*. **2011**, *27*, 465–471 (In Ukrainian). **DOI:**10.7124/bc.000119
26. A.V. Slipkan, D.E. Kytova, A.V. Shtemenko, *Ukr.* Chem. *J.* **2017**, *83*, 35–41 (In Ukrainian).
27. A.V. Slipkan, D.E. Kytova, A.V. Shtemenko, *Voprosy khimii i khimicheskoi tekhnologii*. **2018**, *2*, 39–45 (In Ukrainian).
28. S. Shah, Y. Liu, W. Hu and J. Gao, *J. Nanosci. Nanotechnol.* **2011**, *11*, 919–928. **DOI:**10.1166/jnn.2011.3536
29. H. Maeda and Y. Matsumura, *Adv. Drug. Deliv. Rev.* **2011**, *63*, 129–130. **DOI:**10.1016/j.addr.2010.05.001
30. M. Iziumskyi, S. Melnyk and A. V. Shtemenko *Chem. Met. Alloys*. **2013**, *6*, 121–124. **DOI:**10.30970/cma6.0246
31. B. M. Mosby, A. Diaz, V. Bakhmutov and A. Clierfield, *ACS Appl. Mater. Interfaces*. **2014**, *6*, 585–592. **DOI:**10.1021/am4046553
32. A. Diaz, M. L. Gonzalez, R. J. Perez, A. David, A. Mukherjee, A. Baez, A. Clearfield and J. L. Colon, *Nanoscale,* **2013**, *5*, 11456–1146. **DOI:**10.1039/c3nr02206d

Povzetek

V prispevku poročamo o sintezi kompozita nanodelcev cirkonijevega fosfata (θ-$Zr(HPO_4)_2 \cdot 6H_2O$ (ZrP)), ki vsebujejo spojino renija(III) (*cis*-$Re_2(C(CH_3)_3COO)_2Cl_4 \cdot 2DMSO$ (**I**)). Proces interkalacije smo spremljali z elektronsko absorpcijsko spektroskopijo (EAS). Na osnovi spektroskopskih podatkov smo sklepali, da so ligandi v okolici klastra direnijevega(III) fragmenta razporejeni v *cis* konfiguraciji. V predlaganem mehanizmu interkalacije smo predvideli substitucijo aksialnih ligandov **I** s fosfatnimi skupinami ZrP najprej na površini nanodelcev ZrP, kasneje pa tudi v notranjih plasteh. Dva produkta procesa interkalacije smo karakterizirali z naslednjimi metodami: vrstično elektronsko mikroskopijo (SEM), rentgensko praškovno difrakcijo (XRPD), infrardečo spektroskopijo (FT-IR) in termogravimetrično analizo (TGA). V produktih je bila razdalja med plastmi od 10,53 Å do 16,6 Å, povprečna velikost ploščič pa od 100 nm do 200 nm.